THERMODYNAMIC ANALYSIS OF AN ABSORPTION REFRIGERATION SYSTEM USED TO COOL DOWN THE INTAKE AIR IN AN INTERNAL COMBUSTION ENGINE

R. Novella, V. Dolz[1], J. Martín, L. Royo-Pascual

CMT – Motores Térmicos, Universitat Politècnica de València, Spain

Abstract

This paper deals with the thermodynamic analysis of an Absorption Refrigeration Cycle used to cool down the temperature of the intake air in an Internal Combustion Engine using as a heat source the exhaust gas of the engine. The solution of ammonia-water has been selected due to the stability for a wide range of operating temperatures and pressures and the low freezing point. The effects of operating temperatures, pressures, concentrations of strong and weak solutions in the Absorption Refrigeration Cycle were examined to achieve proper heat rejection to the ambient. Potential of increasing Internal Combustion Engine efficiency and reduce pollutant emissions was estimated by means of theoretical models and experimental tests. In order to provide boundary conditions for the absorption refrigeration cycle and to simulate its effect on engine performance, a 0D thermodynamic model was used to reproduce the engine performance when the intake air is cooled. Furthermore, a detailed experimental work was carried out to validate the results in real engine operation. Theoretical results show how the absorption refrigeration system decreases the intake air flow temperature down to a temperature around 5 °C and even lower by using the bottoming waste heat energy available in the exhaust gases in a wide range of engine operating conditions. In addition, the theoretical analysis estimates the potential of the strategy for increasing the engine indicated efficiency in levels up to 4% also at the operating conditions under evaluation. Finally, this predicted benefit in engine indicated efficiency has been experimentally confirmed by direct testing.

Keywords

Absorption Refrigeration Cycle, Diesel engine, Waste Heat Recovery, alternative solutions, ammonia-water

[1] V. Dolz. CMT-Motores Térmicos, Universitat Politècnica de Valencia, Camino de Vera s/n, 46022 Valencia, Spain. Phone: +34 963877650 Fax: +34 963877659 e-mail: vidolrui@mot.upv.es

NOMENCLATURE

Acronyms

ARC	Absorption Refrigeration cycle
COP	Coefficient of performance
RHE	Refrigerant Heat Exchanger
SHE	Solution Heat Exchanger
WHR	Waste Heat Recovery
ICE	Internal Combustion Engine
ICV	Intake Closing Valve

Notation

Latin

$\dot{m}$	Mass flow rate (kg/s)
C	Specific Heat Capacity (kJ/kgK)
h	Specific enthalpy (kJ/kg)
T	Temperature (°C)
P	Pressure (bar)
Q	Heat Exchangers Power (kW)
W	Pump Power (kW)
v	Specific volume (m^3/kg)
X	Solution concentration

Greek letters

ε	Effectiveness of heat exchanger
η	Isentropic efficiency of the pump

Subscripts

abs	Absorber
$cond$	Condenser
gen	Generator
$evap$	Evaporator
p	Pump
$actual$	Actual process
max	Maximum
min	Minimum
h	High
iso	Isentropic Process
o	Outlet
i	Inlet
ref	Reference state
$high$	High level
low	Low level
SS	Strong solution
WS	Weak Solution
$1-12$	State points

1. INTRODUCTION

Nowadays, different Waste Heat Recovery (WHR) technologies applied in Internal Combustion (IC) engines are under research in order to generate electrical or mechanical energy for the vehicle or to heat specific elements during its warm-up process. According to the Figure 1, these technologies can be classified in different types:

- Heat to heat, this technique consists of installing a heat exchanger on the exhaust line in order to heat up critical zones of the engine during its warm up process. It is relatively easy to implement, however it only has potential during cold starting processes [1].
- Electrical turbocompounding, which consists of an electric generator coupled to a turbocharger. The generator extracts surplus power from the turbine, and the electricity produced is used to run a motor coupled to the engine crankshaft [2][3].
- Mechanical turbocompounding, in this case, the engine is equipped with an additional power turbine. This turbine is placed in the exhaust line and is mechanically coupled to the engine crankshaft via a gearbox [2] [3].
- Rankine cycle, where the vapour is generated from the thermal energy of the exhaust gases using an evaporator. After, this vapor is expanded using an expander machine and generating mechanical power. Particularly, Organic Rankine Cycles (ORC), based on the use of organic fluids, are especially suited to recover energy from exhaust gases at low temperatures [4–7] .
- Other thermodynamic cycles, as Ericsson, Brayton, Stirling, absorption and ejection cycles. Generally, these technologies are less mature than the ORC and they are focused on reducing the ORC complexity and generate an additional mechanical power [8].
- Thermal electricity, which consist of thermoelectric materials installed in the exhaust pipe and generating electricity by Seebeck effect, thus providing at least some of the powertrain electric power requirements. Nowadays, these materials have low efficiency and are expensive so it would be a promising technology if these materials can be improved [9], [10].

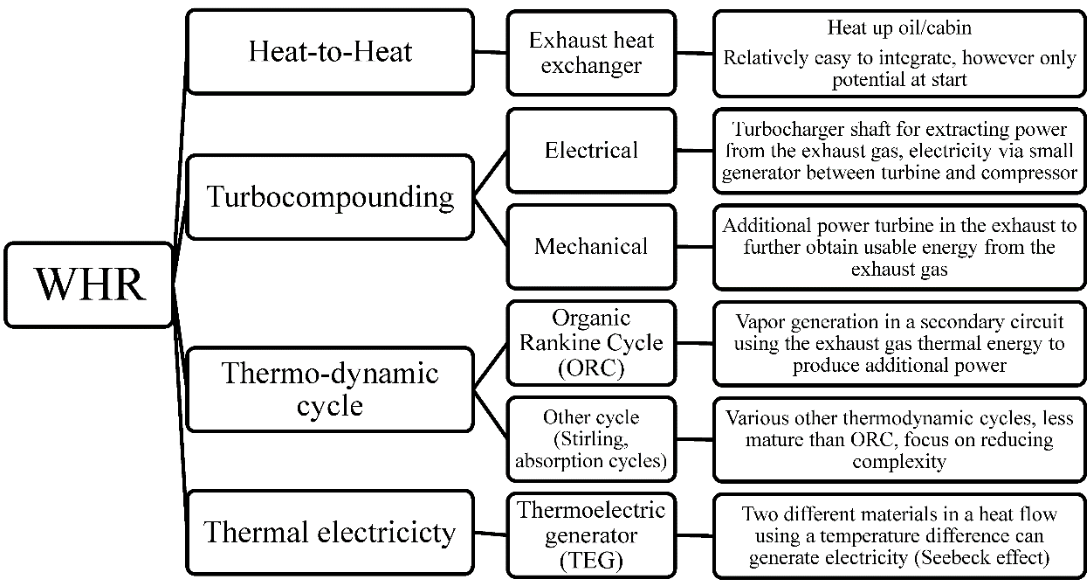

Figure 1. Trends in WHR technologies applied to ICE

The main objective of this study is to estimate the feasibility of a system for recovering heat energy from the exhaust gas, in order to cool the intake air of an IC engine and consequently improve the engine efficiency and reduce pollutant emissions. Considering the previous classification, it would be a new type of WHR system used on a "heat to cool" process. These thermodynamic cycles can be performed as tri-thermal cooling systems (ejection cycles or absorption cycles). On these cycles, the system expels the heat to a fluid at a reference temperature and take the heat from a high temperature source (higher than the reference) and from a low temperature source (lower than the reference). On the present study, the reference temperature is ambient temperature, the high temperature source is the exhaust gas and the low temperature source is the intake air.

Some applications related to replacing air conditioning compression systems with absorption cooling systems on vehicles are common on literature. Some theoretical studies consider different IC engines coupled with absorption units as WHR systems for air conditioning with positive results [11–16]. On these works, cooling powers from 18.4 W to 10 kW and COP coefficients from 4.9% to 80% are obtained. High challenges existed as regards packaging, working fluids (in the case of absorption cycles) and the cost of the system. An estimation of theoretical maximum increment in engine brake thermal efficiency of 2.5% was predicted by Talbi et. al [15]. Moreover, a simulation of a caterpillar engine using the absorption refrigeration unit to cool the air before the intercooler was done by Agnew et al. [14], achieving a theoretical maximum increment in engine brake thermal efficiency of 2%. Jianbo et al. [17] showed that show that the absorption refrigeration sub-cycle can completely meet the space cooling demand (30 kW) for the coach when it runs over 100 km/h, with a COP of 40%. Rêgo et al. [18] tested an experimental installation with an absorption refrigerator driven by automotive exhaust gas heat. Moreover, a system for controlling the refrigeration system heat input was developed.

On the other hand, in 2015, M.T. Zegenhagen and F. Ziegler have published two papers about the viability of cooling the intake air of a turbocharged gasoline engine in order to improve its behavior by using an jet-ejector cooling system [19], [20]. In these works, they use R134a as a working fluid, generating a cooling power between 2.3 kW and 5.3 kW.

Despite of these theoretical and experimental studies, where the absorption cycle has been used to power the air-conditioning in a vehicle, no theoretical or experimental study is available in the literature using the absorption cycle to cool down the temperature of the intake air in an engine. Considering these studies, it is possible to list several advantages of these cycles when they are used to cool the intake air of the IC engine. Some advantageous effects are directly related with this temperature reduction of the intake air:

- An improvement of the volumetric efficiency of the IC engine.
- A reduction in heat losses of the IC engine (thus, an increment in the adiabatic conditions of the engine), due to the reduction of mean temperatures through the engine. This reduction of the heat rejection would increase the indicated efficiency of the engine.
- A diminution in the NOx emissions due to this reduction of mean value of flow temperatures and thus of in-cylinder peak temperatures.

Other advantageous effects indirectly related with this temperature reduction could be obtained modifying the injection settings, piston shapes and optimizing combustion processes to adapt the engine to these lower temperatures of intake air. Finally, the post treatment elements of exhaust line could be simplified due to the reduction in pollutant emissions of the engine.

The objective of the present paper is to estimate the potentiality of intake air cooling using an absorption cycle with the exhaust gases as waste heat source at different working conditions of the engine. The second objective is to estimate the direct advantages of this temperature reduction of intake air on the engine efficiency and pollutant emissions. Finally, a critical discussion is performed about the viability of this system in an actual vehicle.

2. ABSORPTION REFRIGERATION CYCLE MODEL

2.1. Thermodynamic analysis

Figure 2 shows the schematic diagram of an absorption cycle using waste heat energy. As this figure illustrates, it contains a generator, an absorber, a condenser, an evaporator, a solution heat exchanger (SHE) and a refrigerator heat exchanger (RHE) to improve cycle efficiency. It operates as follows: Heat input from the hot source (exhaust gases) (Q_G) evaporates the high pressure solution ammonia-water (point 1) in the generator. The generator separates the inlet flow in two streams. The first one, which corresponds to the ammonia (point 2), leaves the generator at the top side in vapor phase. The second one, which consists of a mixture of water (higher concentration) and ammonia (lower concentration) (point 3) leaves the generator at the bottom in liquid phase. Differences between boiling points of water and ammonia ensure the separation of these two flows. High pressure ammonia vapor stream enters the condenser (reducing its temperature, point 4), where it releases heat to the ambient (Q_C). Liquid ammonia leaves the condenser, through the refrigerator heat exchanger, which improves cycle efficiency (point 11). Consecutively, the ammonia flows through an isenthalpic valve, which reduces its pressure (point 5), reaching the evaporator pressure (low pressure). The ammonia enters the evaporator, receiving heat from the cold source (intake air) (Q_E), increasing low pressure vapor temperature (point 6). At the outlet of the evaporator, the regenerator increases the vapor temperature (point 12). Then, the ammonia enters the absorber, where it is absorbed by the weak solution of water and low concentration of ammonia (point 10). Heat of the absorber should be rejected to the ambient (Q_A); therefore, its temperature should be above to the ambient temperature. The solution with high ammonia concentration (point 7) is pumped to the vapor generator (point 8) through the Solution Heat Exchanger (SHE) (point 1). The weak solution leaves the generator (point 3) and reduces its temperature in the SHE (point 9). Then, the weak solution enters the absorber to absorb ammonia vapor from the evaporator (point 10). Then, the cycle starts again. The Solution Heat Exchanger decreases temperature of the weak solution and increases temperature of strong solution, increasing the cycle coefficient of performance (COP). A pump drives the pumping process, not a compressor, therefore the amount of work required in this cycle is an order of magnitude lower than an ordinary vapor compression cycle. To sum up, using a direct thermal energy from exhaust gases (T High) is possible to cool down the intake air in a vehicle (T Low) releasing heat to the ambient in an intermediate sink (T Medium).

Using the equations describing vapor-liquid equilibrium properties of the ammonia-water system presented by Pátek et. al [18] based on experimental data and the energy relations shown in Table 1 the absorption refrigeration system was simulated.

Table 1. Energy relations for the elements of the absorption refrigeration cycle

Element	Energy relations
Generator	$Q_G = \dot{m}_2 * h_2 + \dot{m}_3 * h_3 - \dot{m}_1 * h_1$
Condenser	$Q_C = \dot{m}_2 * (h_2 - h_4)$
RHE	$\varepsilon_{RHE} = \frac{Q_{actual}}{Q_{max}} = \frac{C_h * (T_4 - T_{11})}{C_{min} * (T_4 - T_6)}, \dot{m}_2 * (h_4 + h_6) = \dot{m}_2 * (h_{11} + h_{12})$
Evaporator	$Q_E = \dot{m}_2 * (h_6 - h_5)$
Absorber	$Q_A = \dot{m}_2 * h_{12} + \dot{m}_3 * h_{10} - \dot{m}_1 * h_7$
Pump	$\eta_p = \frac{W_{P,iso}}{W_P}, W_{P,iso} = \dot{m}_1 * \left(h_{8,iso} - h_7\right), W_P = \dot{m}_1 * (h_8 - h_7)$
SHE	$\varepsilon_{SHE} = \frac{Q_{actual}}{Q_{max}} = \frac{C_h * (T_3 - T_9)}{C_{min} * (T_3 - T_8)}, \dot{m}_3 * h_3 + \dot{m}_1 * h_8 = \dot{m}_3 * h_9 + \dot{m}_1 * h_1$

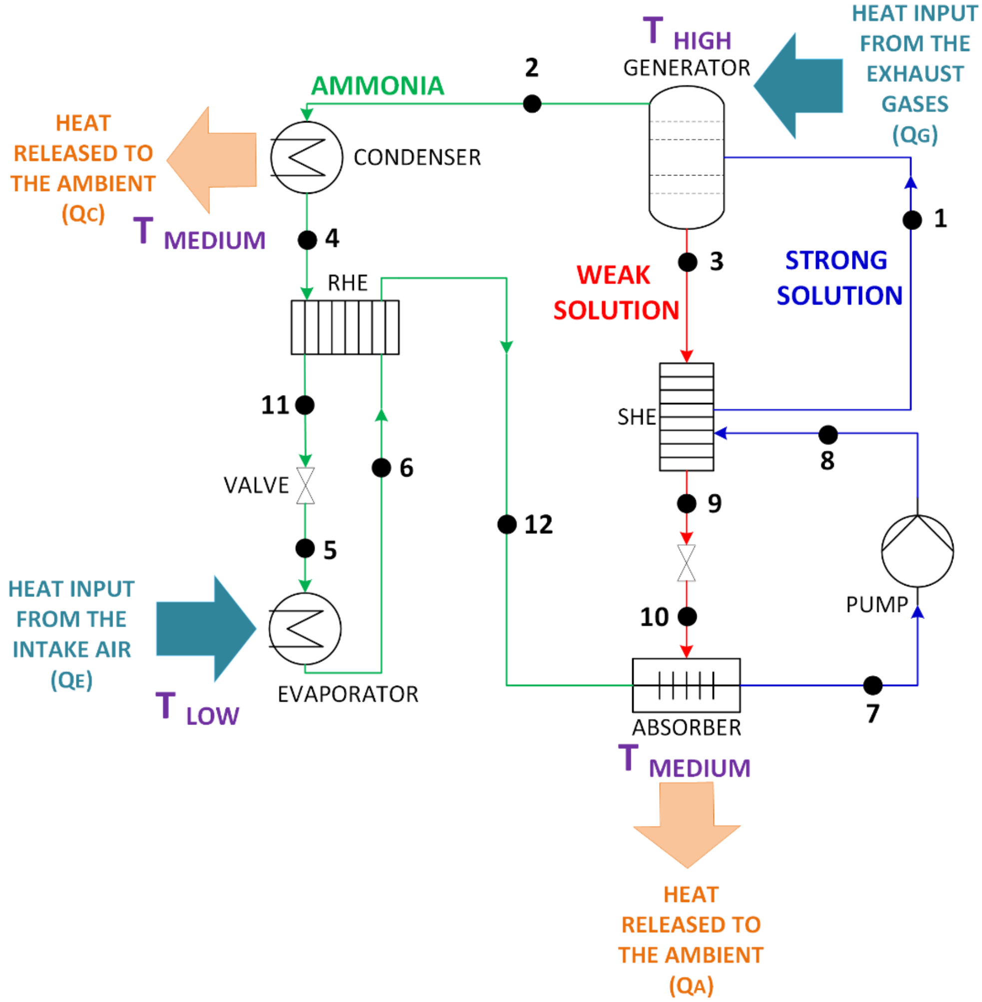

Figure 2. Schematic diagram of absorption cycle

2.2. Limits of the cycle

The following limits were taken into account to define the boundary conditions:

- Temperature in the heat exchangers should be above the ambient temperature to ensure proper heat rejection to the ambient.
- The power release should be the lower as possible to avoid huge sizes of heat exchangers.
- Pressure should be as low as possible to reduce pressure drop through the pipes and to minimize high pipping costs.

2.3. Election of main parameters of the cycle

2.3.1. Solution selection

The most important pairs of solution used in absorption cycles are H_2O-LiBr, NH_3-H_2O, NH_3-$LiNO_3$ and acetone-$ZnBr_2$. Between them, the solution NH_3-H_2O is highly stable for a wide range of operating temperatures and pressures. Moreover, this solution can be used for low temperature applications, as the freezing point of NH_3 is -77°C [19]. However, rectification is required using this type of solution (NH_3-H_2O) to achieve acceptable cycle performance [20]. Therefore, the solution NH_3-H_2O has been used in this absorption cycle. Wang et al. [11] and Mandela et al.

[12] used this solution to recover energy from the exhaust gas of an internal combustion engine to power an absorption refrigeration system and produce the air-conditioning an ordinary passenger car. The American National Standards Institute (ANSI) [24] classified refrigerants into three groups regarding to their safety in use. Ammonia, due to its toxicity, is in group 2, which means that it cannot be used directly in air-conditioning systems in direct expansion in the evaporator coil. Unlike absorption cycles used in air-conditioning, the system presented in section 2.1 has no direct contact with passengers inhabitant space, only with intake air in the engine and the exhaust gases released to the ambient.

2.3.2. Parameters of the cycle

Figure 3 shows the Oldham Diagram of the mixture NH_3-H_2O. In this diagram it can be seen the proportion of ammonia and water in the solution as a function of temperature and pressure at equilibrium. The main parameters that should be defined in the cycle are the high level of pressure in the cycle (P_{high}), the low pressure in the cycle (P_{low}) and the concentration of ammonia (and thus the water) in the weak (X_w) and strong solution (X_r). The following points summarize its impact in the thermodynamic characteristics of the cycle (Figure 3):

- Temperature of the generator (T_G)

The level of high pressure (P_{high}) and the concentration of the weak solution (X_w) define the high temperature of the generator (T_G). It should be taken into account that exhaust gases should contain enough power to evaporate the ammonia.

- Temperature in the evaporator (T_E)

The intersection of the low pressure level (P_{low}) in the cycle and the line of 100% NH_3 define the low temperature in the evaporator (T_E). This temperature will have an effect on the cooling power obtained from this absorption cycle.

- Temperature in the condenser (T_C)

The intersection of the high pressure level (P_{high}) in the cycle and the line of 100% NH_3 leads to the definition of the medium temperature in the condenser (T_C). This temperature should be above ambient temperature to ensure proper rejection to the ambient.

- Temperature in the absorber (T_A)

The level of low pressure (P_{low}) and the concentration of the strong solution (X_r) define the medium temperature in the absorber (T_A). This temperature should be above ambient temperature to ensure proper rejection to the ambient.

Considering the example of Figure 3, high pressure (P_{high}) is 20 bar, low pressure (P_{low}) is 3 bar, the strong solution (X_r) is 40% (40% of ammonia and 60% of water) and the weak solution (X_w) is 15%. Using this values, the following temperatures were obtained in the absorption cycle: Evaporator temperature (T_E) of -10 °C, absorber temperature (T_A) of 41 °C, condenser temperature (T_C) of 48 °C and generator temperature (T_G) of 165 °C.

In order to optimize and fulfill the thermodynamic requirements, the variation of these parameters are presented in section 4 of this paper.

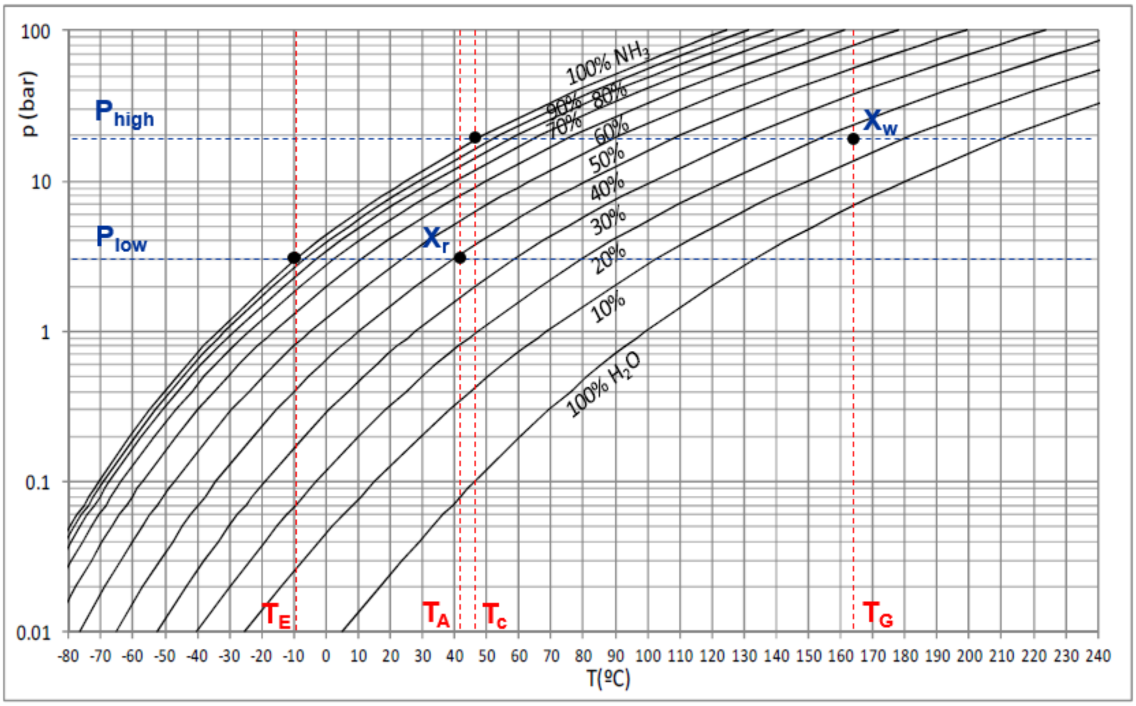

Figure 3. Oldham diagram

2.4. Assumptions

In the system model, the following assumptions were made:

1. The system is operated in steady-state conditions.
2. The refrigerant is saturated at the outlet of the evaporator and the condenser.
3. At the outlet of the absorber and evaporator, solutions are at equilibrium.
4. Thermal and pressure losses were neglected.
5. Effectiveness of Refrigerant Heat Exchanger (RHE) and Solution Heat Exchanger (SHE) are 0.7.
6. The isentropic efficiency of the pump is 0.8.
7. The absorption cycle rejects heat to the ambient by the absorber and the condenser.
8. The system absorbs heat from the cold source (Intake air) and the hot source (Exhaust gases) and reject through the condenser and the absorber to the ambient.
9. No rectification process are included.
10. Temperature at heat exchanger should be above 45°C to ensure proper rejection at extreme conditions.
11. Pinch point in the evaporator is assumed 10°C [25].
12. Optimization process have been made in the point of 4000 rpm and full load.
13. The reference environmental state is assumed T_{ref}=25°C and P_{ref}=1.013 bar.

3. ENGINE EXPERIMENTAL AND MODELING TOOLS

In order to provide boundary conditions for the absorption refrigeration cycle optimization and to simulate its effect on engine performance, a 0D thermodynamic model was used to reproduce the engine performance when the intake air is cooled. Using a simulation tool is very convenient for this research since it helps the designing process of the absorption keeping realistic conditions, and at the same time avoiding the limitations and uncertainties of experimental measurements. Thus, three extreme engine conditions will be considered to evaluate the thermodynamic viability of the absorption cycle taking into account the effect on engine operation (changes on air flow and intake and exhaust conditions). The starting points for the simulation are the three operation conditions measured in the experimental facility described in the next subsection. Starting from the real conditions, the effect of intake cooling will be modeled according to the absorption cycle requirements, with the aim of coupling the thermodynamic characteristics of both the refrigeration and engine cycles.

Finally, once the thermodynamic viability was confirmed, a detailed experimental work was carried out to validate the results in real engine operation.

The experimental facility used to obtain the boundary conditions for the simulations and to validate the results, and thr 0D thermodynamic model are described in next subsections.

3.1. Experimental Facility

The experimental work was performed in a EU4 DI Diesel Engine, whose main characteristics are included in Table 2. Some modifications were carried out in the original engine systems to achieve a better control of the engine parameters and to perform the experimental measurements. Hence, the original coolant and oil circuits were adapted to measure the heat rejection to the coolant, block oil and turbocharger oil independently.

Table 2. Engine technical data

Cylinder	4 in-line
Stroke	4
Bore	75 mm
Unitary displacement	390 cm^3
Total displacement	1560 cm^3
Compression ratio	16:1
Air management	Turbocharged
Maximum power	82 kW - 3600 rpm
Maximum torque	270 Nm - 1750 rpm
Cycle	Diesel
Injection	Common rail

Apart from the engine control systems, the test cell includes specific instrumentation for the detailed heat rejection analysis. The technical characteristics of the test cell instrumentation are presented in Table 3 while the sketch of the test cell is shown in Figure 4. The facility was prepared to acquire the standard data necessary to perform the combustion diagnosis and modelling the internal heat rejection terms [26], and also to measure the data required to complete a global thermal balance of the engine. Therefore, the in-cylinder pressure, some mean variables such as air and fuel mass flows, gas temperatures and pressures at different intake and exhaust positions, and the liquids (oil and coolant) mass flow and temperatures, were measured.

Table 3 Test cell instrumentation

Variable	Equipment
Cylinder pressure	AVL GH13P
Speed	Dynamometer
Torque	Dynamometer
Air mass flow	Sensiflow DN80
Fuel flow	AVL 733S Fuel meter
Fluids temperatures	K-type thermocouples and RTDs
Mean pressure	Kistler Piezoresistive Pressure Transmitters
Gases analysis	Horiba Mexa 7100 DEGR
Coolant flow	Krohne 4010 Optiflux
Oil cooler water flow	Isoil MS500
Fuel cooler water flow	Yoko AdmagAE2018MG
Turbo oil flow	Krohne Optimass 3050C

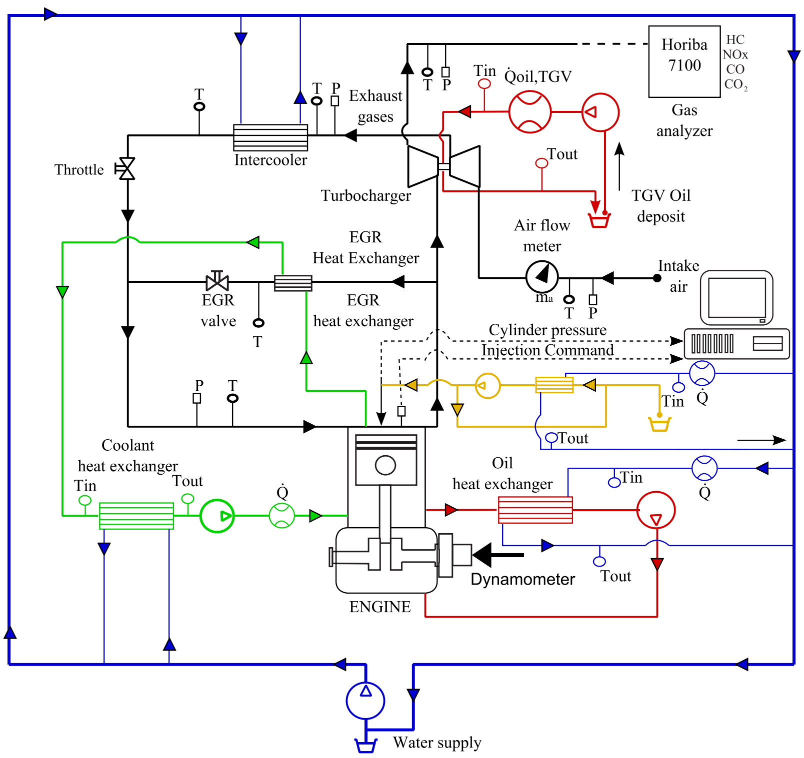

Figure 4 Test cell scheme

The in-cylinder pressure, which is the main input for the calculation of the heat rejection in the chamber and the engine performance, was measured with an AVL GH13P piezo-electric transducer installed at the glow plug hole of each cylinder. The signal provided by the piezo-electric transducer was conditioned by means of a Kistler 5011B amplifier and the digital processing was performed following the method described in [27]. To ensure the accuracy of the pressure signal obtained, the pressure sensor was calibrated according to the traditional method proposed in [28].

Most relevant characteristics (regarding engine fluids) of the three engine conditions used to evaluate the thermodynamic viability of the refrigeration cycle and to simulate its effect are shown in Table 4. These points corresponds to conventional points of the engine map at extreme high and low engine speed and load. The original injection and air management setting in the ECU were used. The name of the tests in the first column means engine speed[rpm]- engine load[% of the maximum load] percentage.

Table 4 Measured points for teh simulation

	m_a [g/s]	m_f [g/s]	T_{cool} [°C]	T_{oil} [°C]	T_{intake} [°C]	$T_{exhaust}$ [°C]
1000 [rpm]-100[%]	16.4	1.03	85.4	92.5	29.4	528.8
4000[rpm]-25[%]	74.7	1.68	85.7	98.1	30.9	374.1
4000[rpm]100[%]	113.3	5.11	85.8	126.2	35.4	685.6

3.2. 0D thermodynamic engine models

During the present study two 0D single-zone thermodynamic models (CALMEC and siCiclo) were used. Both of them share the same main hypothesis in order to keep the consistency of the analysis:

1. Chamber pressure and temperature are assumed to be spatially uniform.
2. Three species (air, fuel vapor and stoichiometric combustion products) are considered [26].
3. Ideal gas law is used to calculate gas mean temperature.
4. A filling and emptying model is used to calculate the processes during intake and exhaust strokes, the effect of intake cooling on them and thus on trapped conditions [27].
5. Specific heat of the gas depends on both temperature and composition [28].
6. Instantaneous blow-by leakage is calculated with a model based on the isentropic nozzle flow [26].
7. Chamber volume deformation is calculated by means of a simple deformation model [29].
8. Heat transfer to the chamber walls is calculated with a modified Woschni-like model [30].

A main issue for evaluating the effect of temperature reduction on engine performance, is the calculation of in-cylinder heat rejection to chamber walls. Besides the tuned convective heat transfer model based on the Woschni's proposal, a lumped conductance model was used to calculate wall temperatures in the chamber and ports along with the heat rejection repartition to coolant (from liner and cylinder-head) and oil (from piston). It consists of 102 nodes in the cylinder head, 66 in the liner, 10 in the piston and some boundary nodes that take into account the oil, coolant, fresh air, in-cylinder gas, and intake and exhaust gases. More details of this model are provided in [31].

An in-house methodology [32] was implemented to determine some experimental uncertainties related to in-cylinder pressure (pressure pegging and TDC position) along with some engine characteristics (dynamic and static compression ratios and HT convective model adjustment).

CALMEC is the combustion analysis tool developed to calculate the RoHR from the instantaneous evolution of in-cylinder gas properties by solving the 1st law of thermodynamics in the chamber and modelling the internal thermal flows based on the instantaneous pressure evolution.

SiCiclo [26] is a predictive tool that, using the RoHR as main input, is able to calculate the pressure evolution with the purpose of predicting engine performance and fuel consumption or obtaining boundary conditions for specific combustion models with higher computational requirements [33, 34] and in this case for the absorption cycle model. SiCiclo takes into account all the relevant engine subsystems through the combination of both physical and semi-empirical submodels to calculate the heat transfer flows to combustion chamber walls and ports, split of mechanical losses and intake and exhaust processes [23].

4. RESULTS AND DISCUSSION

Two analysis decoupled are presented in this point. On one side, the optimization of the main parameters of the absorption refrigeration cycle are analyzed (High pressure, Low pressure, concentration of strong and weak solution). Using the optimization analysis, final values of the main parameters of the cycle are obtained taking into account the worst operating point regarding engine cooling conditions (4000[rpm]-100[%]).

On the other hand, absorption cycle is a suitable method for increasing engine efficiency through the intake charge cooling below ambient temperature, thus increasing power density and engine efficiency, or decreasing mechanical stress (because the same trapped gas can be achieved with a lower intake pressure). Moreover, additional benefits in terms NOx reduction, main issue in Diesel engines, can also be obtained. Although in the sake of brevity, the detailed analysis of all these advantages cannot be dealt with in this work, a theoretical estimation of the impact on the particular engine and operating conditions used to design the absorption cycle is presented. Moreover, the experimental assessment of the cooling effect during the real engine operation was also evaluated.

4.1. Optimization of the absorption refrigeration cycle

In order to understand and optimize the cycle for this particular application, several sensitivity studies have been performed varying the main parameters of the absorption cycle, which are the high pressure, the low pressure and the concentration of weak and strong solution. In each subsection one parameter was varied and the rest remained constant. The ranges of the variables in these sensitivity studies are presented in Table 5 and explained in section 4.1.1, 4.1.2 and 4.1.3.

Table 5. Summary of the sensitivity study

Variable	Sensitivity study 1	Sensitivity study 2	Sensitivity study 3
P high [bar]	10-20	17.95	17.95
P low [bar]	4	2-10	4
Xw [%]	0.15	0.15	0.1-0.25
Xr [%]	0.39	0.39	0.3-0.45

4.1.1. High pressure

High pressure was varied in this subsection. As shown in

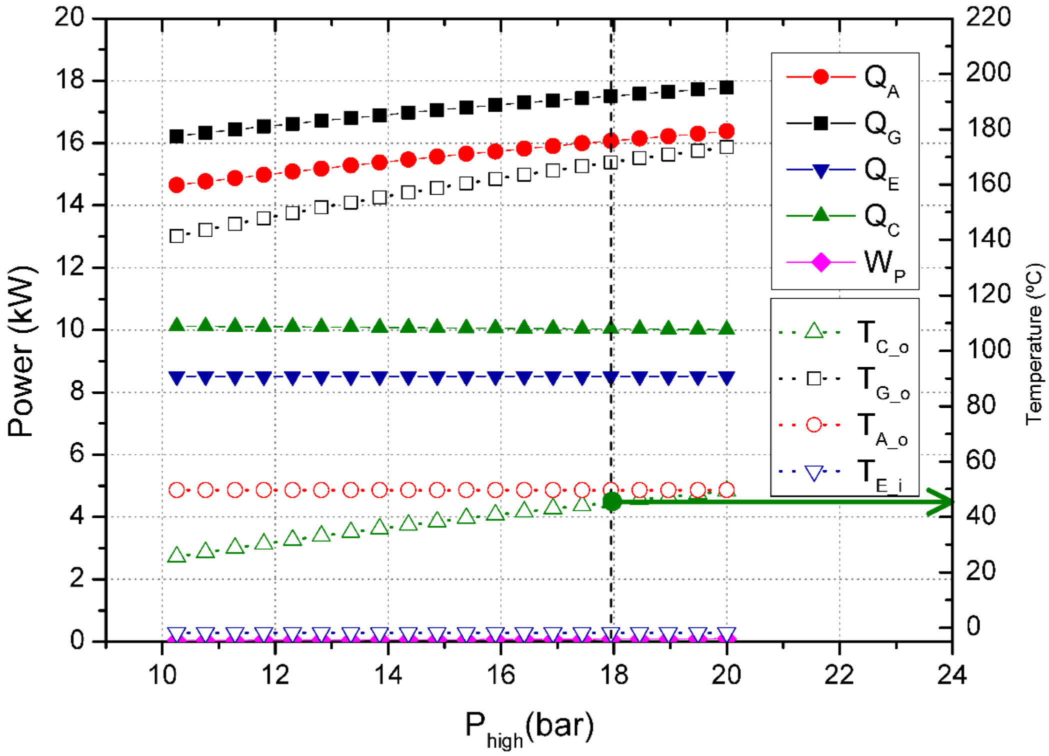

Figure 5, power of the evaporator (Q_E), condenser (Q_C) and pump (W_P) remains approximately constant. However, power in the generator (Q_G) increases because more heat is needed at high pressures to evaporate the solution and produce ammonia. As power in the generator increases and the rest remains constant, it is needed more heat to reject in the absorber (Q_A) to keep the global energy balance. Regarding temperatures (right axis) four values have been plotted, i.e. temperature at the outlet of the generator (T_{G_o}), temperature at the outlet of the condenser (T_{C_o}), temperature at the outlet of the absorber (T_{A_o}) and the temperature at the inlet of the evaporator (T_{E_i}). Temperature at the outlet of the absorber remains constant due to equilibrium assumption. As it can be seen, both temperature at the outlet of the generator and the condenser increase with high pressure. Temperature at the inlet of the evaporator remains also constant because it depends only on the low pressure level. Higher temperatures at the outlet of the generator imply greater power rejection to the ambient. Power rejection in the condenser should be to the ambient; therefore, it should be above 45°C to ensure proper heat release even at summer in warm areas. Thus, high pressure should be the minimum pressure possible in order to minimize the heat transferred from the exhaust gases, but as high as possible in order to ensure proper heat rejection to the ambient. Therefore, the high pressure level was fixed to 17.95 bar.

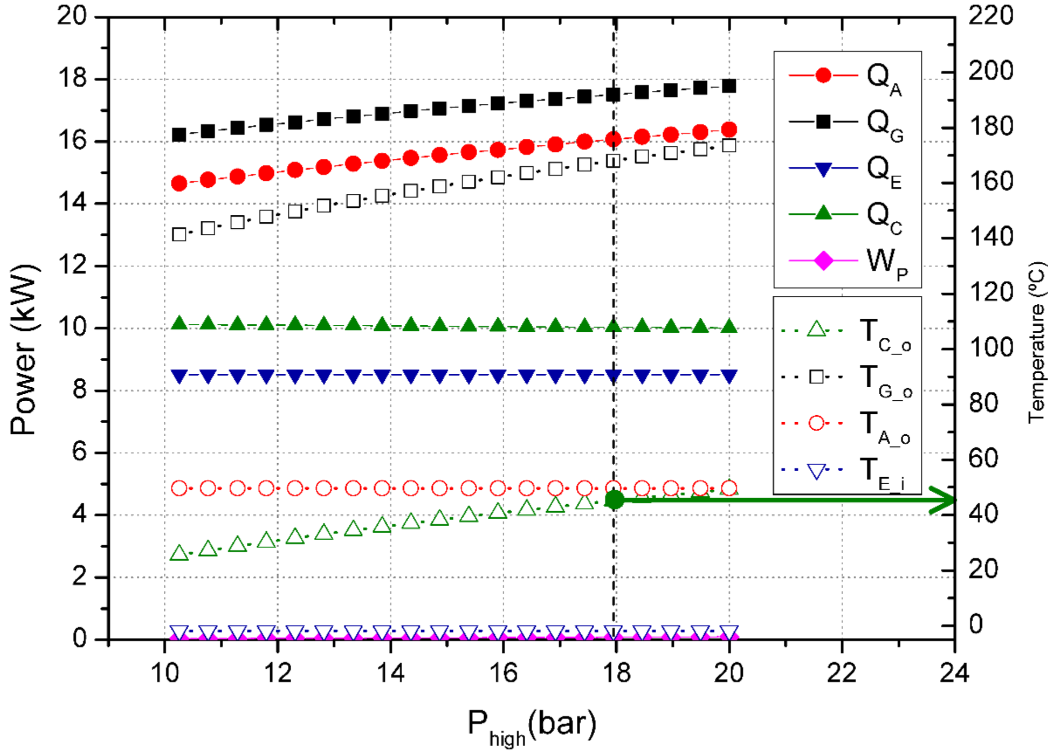

Figure 5. Variation of powers and temperatures with P high

4.1.2. Low pressure

Low pressure was varied in this subsection. As shown in

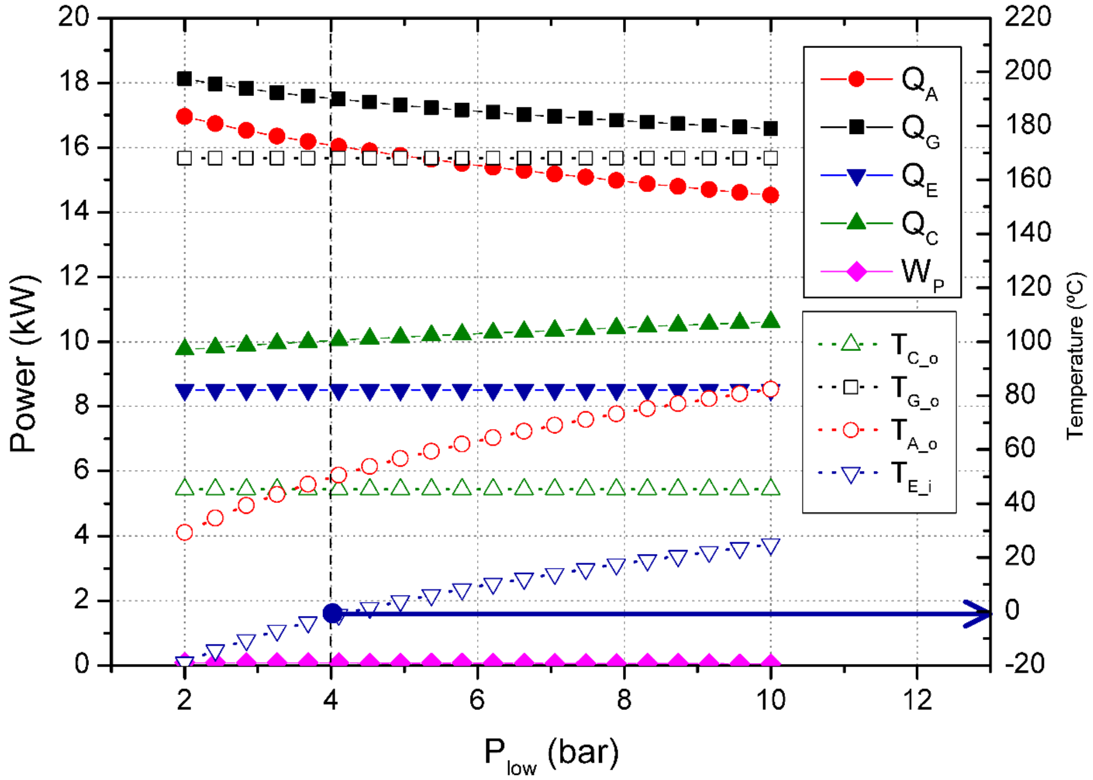

Figure 6, power of the evaporator (Q_E) and pump (W_P) remains approximately constant. Power in the generator (Q_G) and the absorber (Q_A) decreases with higher low pressures because less heat is needed at high low pressures to evaporate the solution and produce ammonia due to the fact that both pressure levels are nearer (as seen in Figure 3). Power in the absorber decreases more than in the generator, therefore power in the condenser slightly increases to keep the global energy balance. Regarding temperatures (right axis) four values have been plotted, i.e. temperature at the outlet of the generator (T_{G_o}), temperature at the outlet of the condenser (T_{C_o}), temperature at the outlet of the absorber (T_{A_o}) and temperature at the inlet of the evaporator (T_{E_i}). Temperature at the outlet of the generator and the condenser remains constant due to small differences in the level of high pressure. As it can be seen in Figure 3, both temperature at the outlet of the absorber and the inlet of the condenser increase with higher low pressure when the strong concentration is fixed. Lower temperatures at the inlet of the evaporator imply greater absorption power in the intake air. However, intake air should not been reduced below 0°C to avoid freezing the content of water in humid intake air and produce problems in the intake line. Therefore, considering 10°C as an objective temperature of intake air and a pinch point of 10°C the temperature at the inlet of the evaporator should be below 0°C to ensure proper heat transfer process. On the other hand, low pressure should be as high as possible, in order to minimize the heat rejection to the ambient. Thus, low pressure should be below 4.5 bar. In this case, it was fixed to 4 bar.

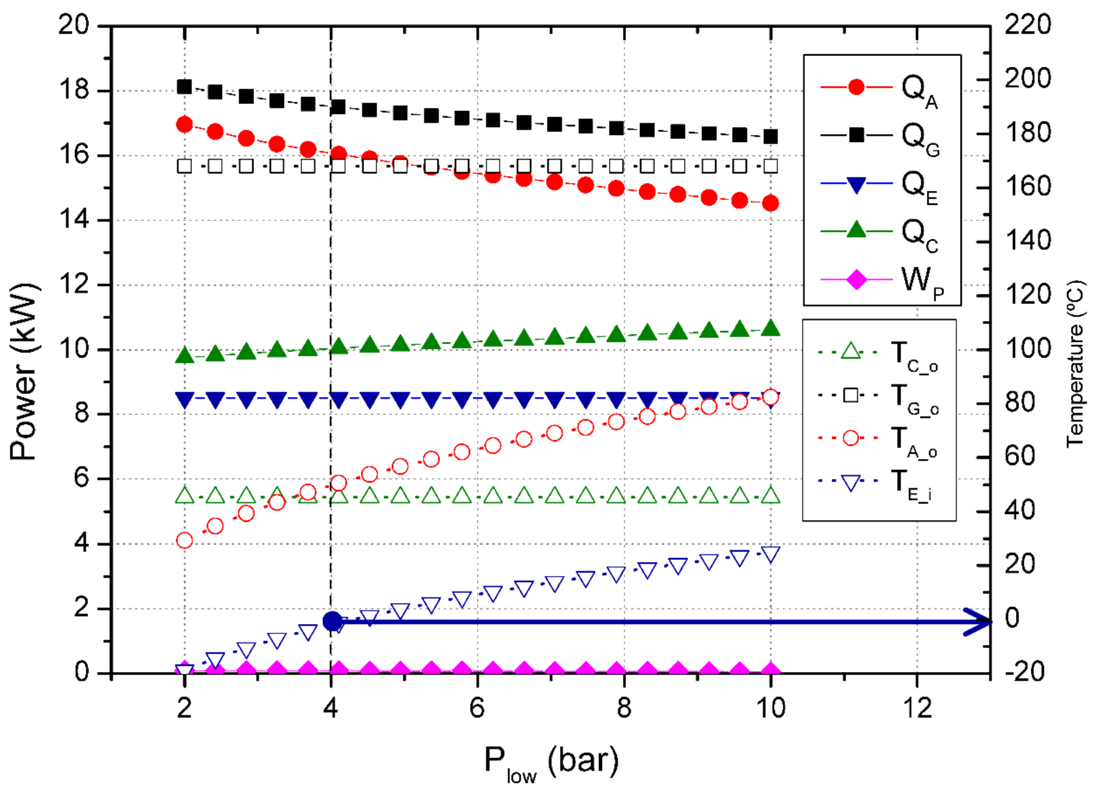

Figure 6. Variation of powers and temperatures with P low

4.1.3. Concentration of weak and strong solution

Concentration of weak and strong solution were varied in this subsection. As shown in Figure 3 the relation between low pressure and the strong solution determines the temperature in the absorber. Therefore, the *concentration of strong solution has an effect on the temperature at which heat should be rejected.*

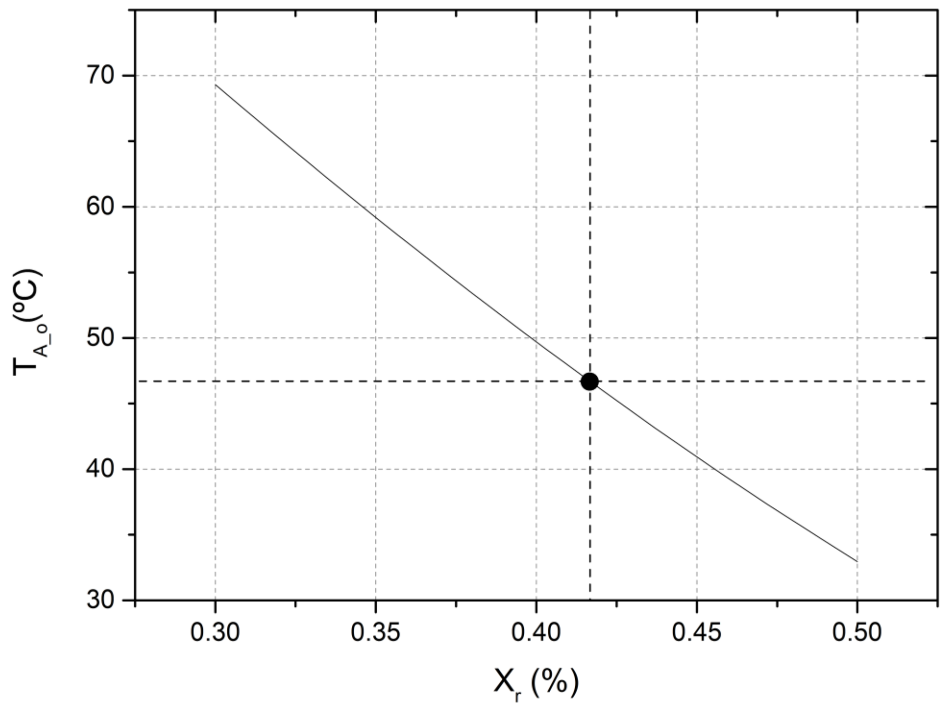

Figure 7 shows the variation of temperature at the outlet of the absorber as a function of strong concentration solution. Concentration of weak solution does not have any effect on this temperature, thus, it has not been taken into account. As previously presented, temperature of heat rejection should be above 45°C to ensure proper heat rejection. Thus, strong concentration should be below 0.42 (42% ammonia-58% water).

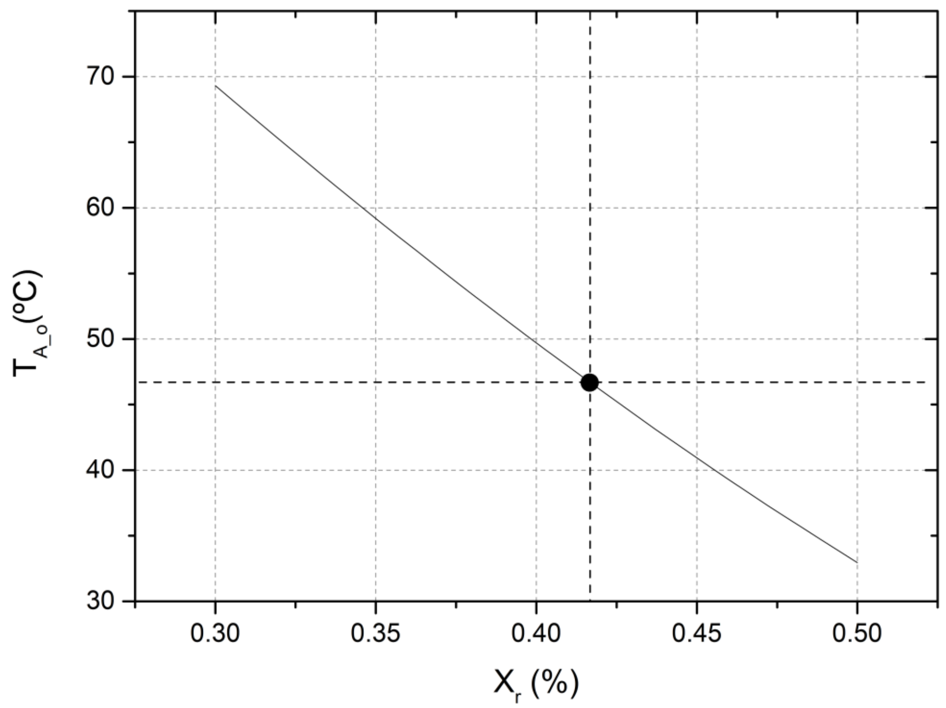

Figure 7. Variation of temperature at the outlet of the absorber vs strong concentration

In order to optimize the election of both concentrations, heat rejection in the absorber and condenser were plotted. Figure 8 shows the power rejected in the absorption cycle, i.e. the sum of heat in the absorber and in the condenser as a function of weak and strong solution concentration. As shown in Figure 8, the blue area corresponds with lower heat rejection to the ambient, therefore lower size of heat exchanger. This feature is essential to guarantee a compact system.

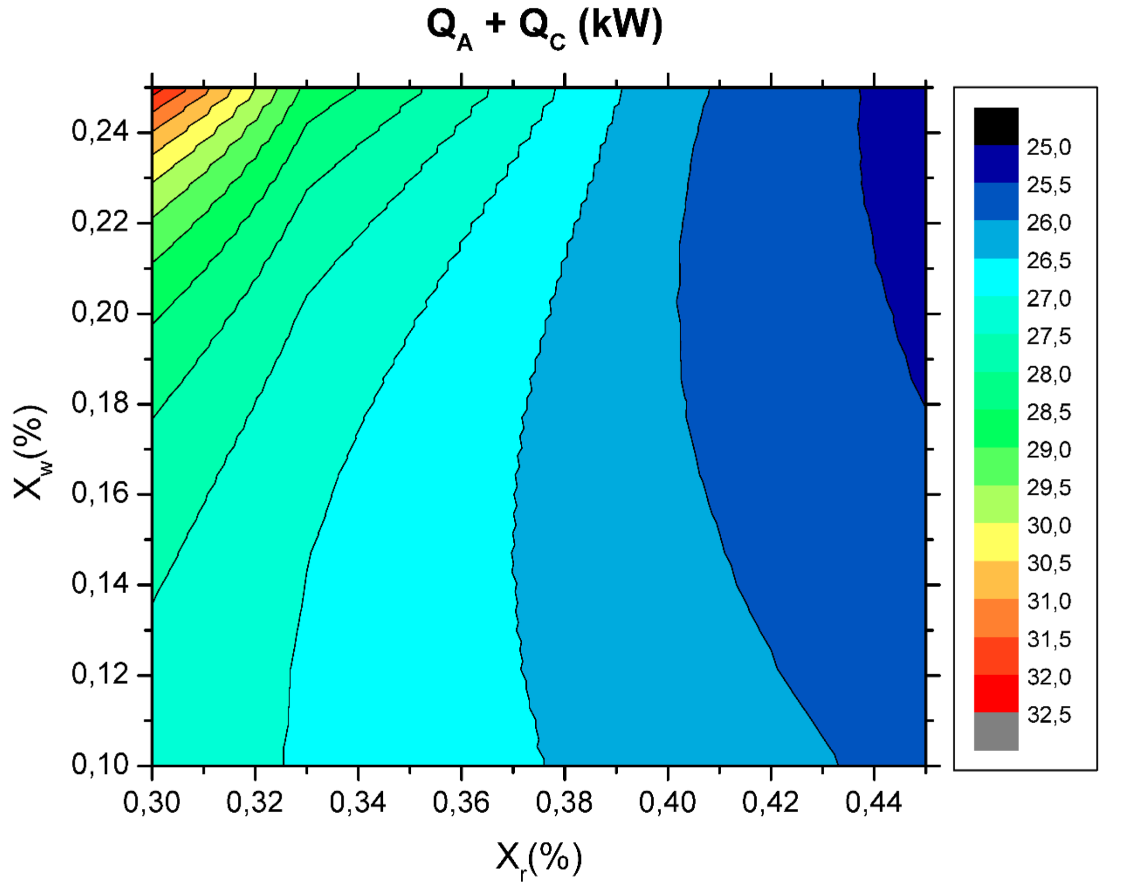

Figure 8. Heat rejection in the absorber vs weak and strong concentration

As there is enough power in the exhaust gases and heat in the evaporator depends on the engine operating point (intake air mass flow) the optimization of this system is based on heat rejection to the ambient. Therefore, the optimization of this system focuses on size and simplicity, not in COP. Figure 9 shows the strong solution mass flow (m_1) as a function of weak and strong concentration. It can be seen a similar behavior as Figure 8. Higher concentration of strong solutions implies lower mass flow rates though the installation. Therefore, it will be needed smaller pipes to provide the required mass flow. The ammonia mass flow will depend on the engine operating point and the required heat absorption in the intake air.

Considering restrictions of temperature at the outlet of the absorber (

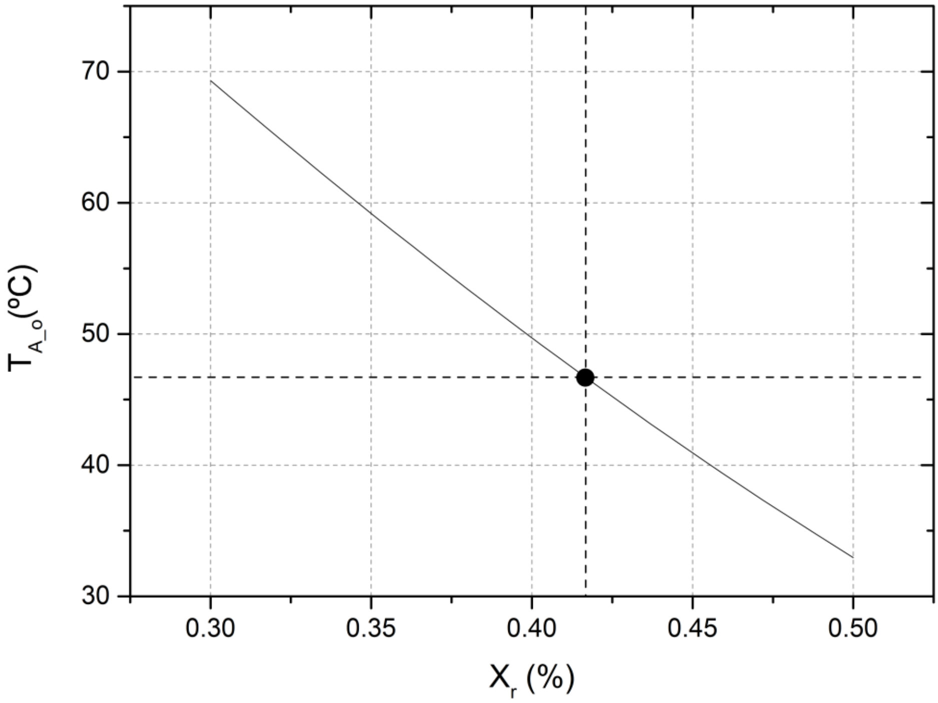

Figure 7), lower heat rejection (Figure 8) and lower mass flow rates through the installation, the following concentrations were selected: X_r=0.39 (39% ammonia-61% water) and X_w=0.15 (15% ammonia-85% water). All of them accomplish the estimated requirement of a concentration below 0.42 in order to ensure a heat rejection to the ambient.

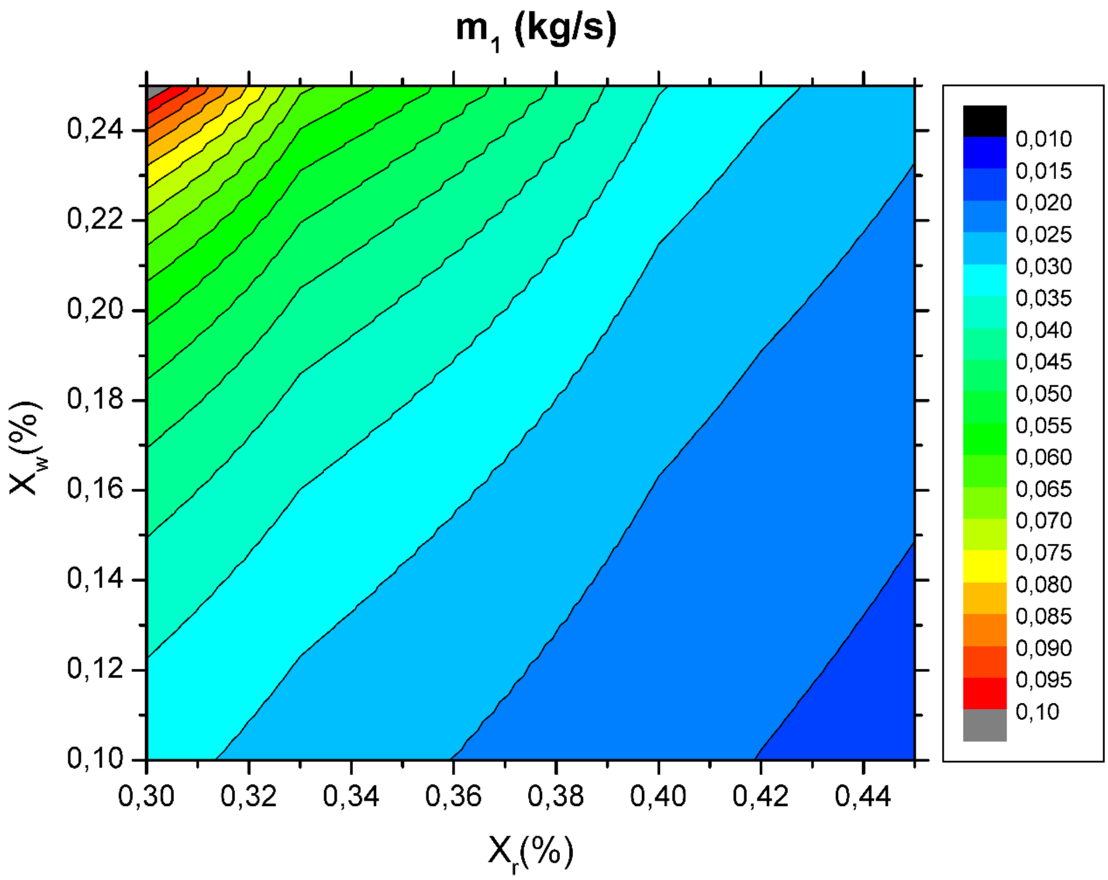

Figure 9. Strong solution mass flow vs weak and strong concentration

Considering parameters optimized in previous chapters, all the parameters of the cycle have been calculated. Table 6 list the calculated values of mass flow rates, pressure, temperature, ammonia concentration, enthalpy, entropy and specific volume at different points of the absorption refrigeration cycle used to cool down the intake air of an ICE.

Table 6. Operating conditions for the absoption refrigeration cycle.

State no.	m_i[kg/s]	P_i[bar]	T_i[°C]	X_i[%]	h_i[kJ/kg]	s_i[kJ/kgK]	v_i[m^3/kg]
1	0.02507	17.95	109.1	0.39	264.2	1.36	0.001283
2	0.007078	17.95	168	1	1835	6.02	0.1147
3	0.01799	17.95	168	0.15	625.7	2.081	0.001241
4	0.007078	17.95	45.26	1	416.8	1.726	0.001752
5	0.007078	4	-1.891	1	257.8	1.213	0.0177
6	0.007078	4	-1.891	1	1460	5.646	0.3094
7	0.02507	4	51.55	0.39	2.198	0.6222	0.001182
8	0.02507	17.95	52.1	0.39	5.419	0.6271	0.001182
9	0.01799	17.95	86.88	0.15	265.1	1.179	0.00111
10	0.01799	4	87.11	0.15	265.1	1.183	0.001111
11	0.007078	17.95	12.26	1	257.8	1.199	0.001607
12	0.007078	4	64.03	1	1619	6.172	0.4008

Figure 10 and Figure 11 shows the Oldham diagram of the mixture NH_3-H_2O and the Ammonia Molier Diagram particularized for operating conditions of Table 6.

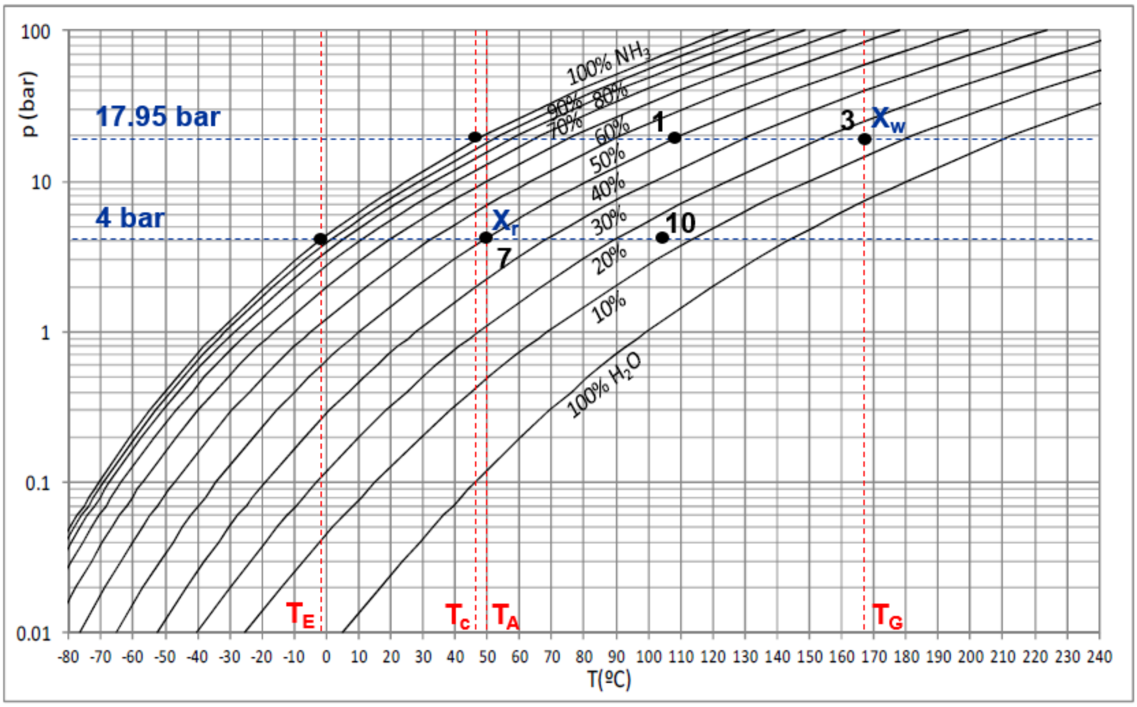

Figure 10. Oldham diagram particularized for operating conditions of the ARC

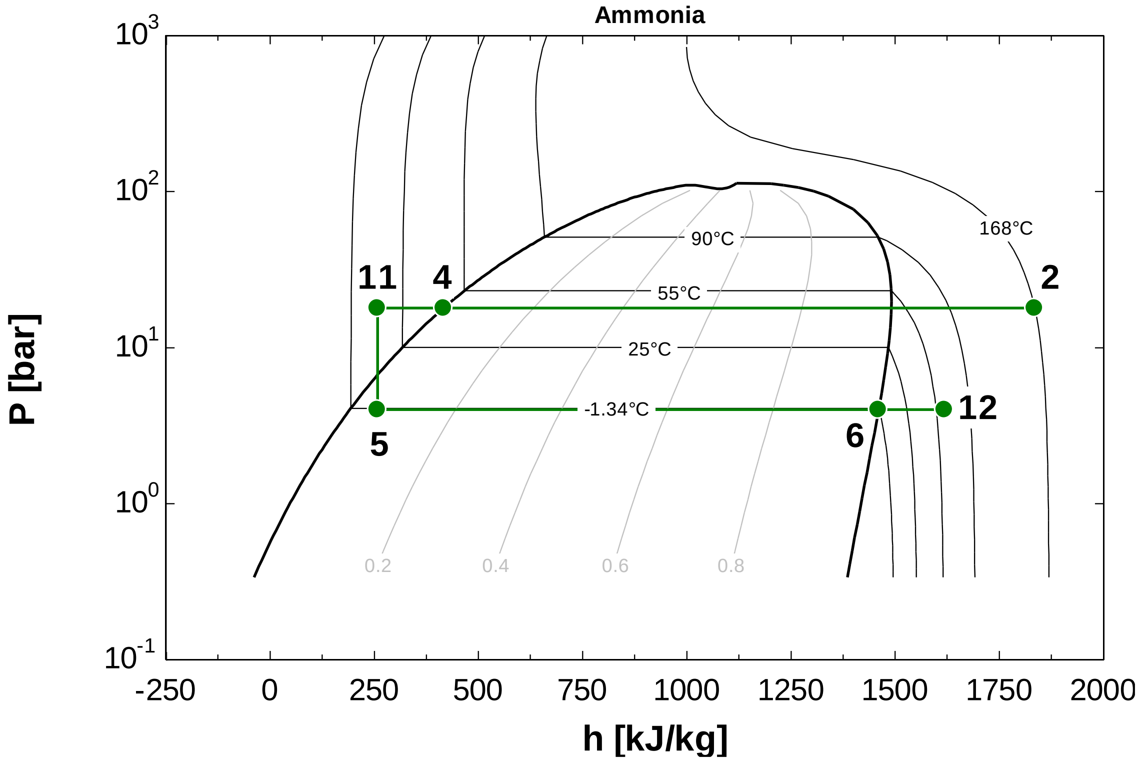

Figure 11. Ammonia Molier diagram particularized for operating conditions of the ARC

4.2. Simulation results

This study was performed for different decrease of temperature (ΔT) in the intake (15°C, 30°C and 65°C) to evaluate the thermodynamic viability of the cycle. By means of reducing temperature from a real engine operating condition, different parameters were analyzed:

- Heat absorbed from the intake air flow
- Heat required from the exhaust gas flow
- Total heat rejected to the ambient

Using equations presented in Table 1 and optimization parameters described in chapter 4, the following results have been obtained. CALMEC diagnosis code was used to obtain the RoHR at the engine operating conditions detailed in Table 4 and then, SiCiclo allowed to simulate the effect of intake cooling on engine performance. Thus, the physically correct sensitivity of the engine related parameters due to the intake ΔT reduction was obtained. Form this data, the required evaporation power was finally estimated. From evaporation power and parameters optimized, the powers remained (pump, generator and absorber) have been solved. Results are shown in Figure 12 are plotted in Figure 13. The name of the tests in the first column means engine speed[rpm]-engine load[% of the maximum load] percentage.

ΔT_{intake_air}=65 °C

	Q_E [kW]	W_P [kW]	Q_G [kW]	Q_A+Q_G [kW]
1000[rpm]-100[%]	1,038	0,00985	2,15	3,198
4000[rpm]-25[%]	5,791	0,05493	11,99	17,830
4000[rpm]-100[%]	8,51	0,08073	17,62	26,210

ΔT_{intake_air}=30 °C

	Q_E [kW]	W_P [kW]	Q_G [kW]	Q_A+Q_G [kW]
1000[rpm]-100[%]	0,4354	0,00413	0,9013	1,341
4000[rpm]-25[%]	2,421	0,02296	5,011	7,454
4000[rpm]-100[%]	3,548	0,03366	7,346	10,930

ΔT_{intake_air}=15 °C

	Q_E [kW]	W_P [kW]	Q_G [kW]	Q_A+Q_G [kW]
1000[rpm]-100[%]	0,2047	0,001942	0,4238	0,631
4000[rpm]-25[%]	1,109	0,01052	2,295	3,414
4000[rpm]-100[%]	1,62	0,01537	3,354	4,989

Q_E: Heat absorbed from the intake air
W_P: Power required by the pump
Q_G: Heat absorbed from the exhaust gases
Q_M=Q_A+Q_C: Heat released to the ambient

Figure 12. Powers of ARC elements of different engine operating points

The three engine operating points (1000[rpm]-100[%], 4000[rpm]-25[%] and 4000[rpm]-100[%]) and four absorption refrigeration powers (Q_E, Q_M (Q_A+Q_C), Q_G and W_P) are presented. As expected, it can be seen that points of 4000 rpm and 100% load require the higher power rejected to the ambient due to higher air mass flows in the intake system. At this point, the heat rejected to the ambient will be 26 kW if a temperature difference of 65°C is required.

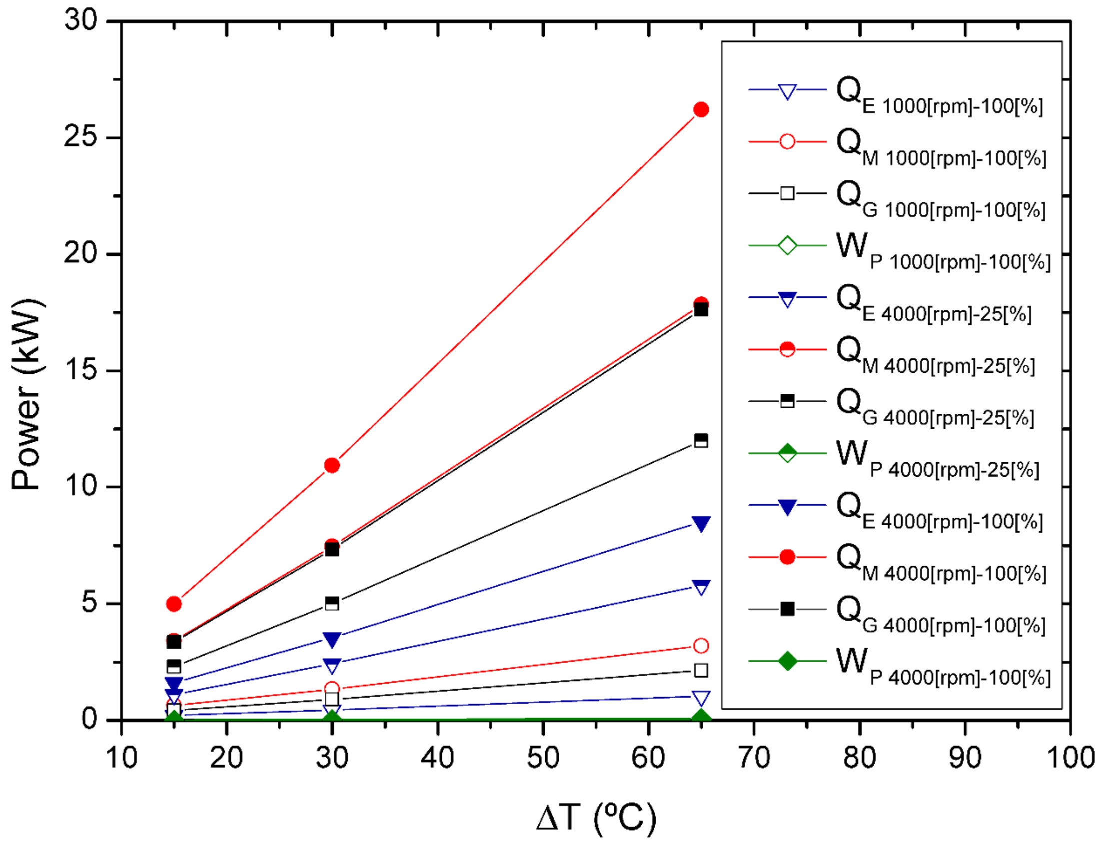

Figure 13. Power rejected and absorbed by the cycle vs deltaT intake air

Table 7 shows the relation between heat rejected in the absorber and condenser and exhaust gases power (considering T_{ref} and P_{ref} as reference state). It can be seen that using 42% of the exhaust gases in the worst case the refrigeration requirements could be fulfilled. Therefore, it can be concluded that this system could reduce the intake air temperature without restrictions.

Table 7. Relation between PEG and heat rejection for engine operating points

Engine operating point	ΔT [°C]	Q_M [kW]	P_{EG} [kW]	Q_M / P_{EG}
4000[rpm]-25[%]	65	2.15	12.43526	17%
4000[rpm]-25[%]	30	0.9013	12.58927	7%
4000[rpm]-25[%]	15	0.4238	11.77716	4%
4000[rpm]-100[%]	65	11.99	28.81002	42%
4000[rpm]-100[%]	30	5.011	30.16750	17%
4000[rpm]-100[%]	15	2.295	31.17210	7%
1000[rpm]-100[%]	65	17.62	84.17066	21%
1000[rpm]-100[%]	30	7.346	86.09373	9%
1000[rpm]-100[%]	15	3.354	87.57280	4%

4.3. Impact on engine efficiency

The 0D engine thermodynamic model described in Section 3 was used to simulate the impact of intake temperature on key air management parameters, thermomechanical loads in the chamber, heat transfer through the chamber walls, heat rejected with the exhaust gases and engine indicated efficiency at the three engine operating conditions. The trends predicted by the model will be later experimentally validated to confirm the observed effects, however the operating conditions and the range of variation of the intake temperature were adapted according to the experimental facility, as detailed below.

Figure 14 (left) confirms the expected effect of T_{intake} on T_{IVC} (Temperature at Inlet Valve Closing Angle) since they are linearly related, so the temperature of the trapped mass decreases significantly. As a result, m_{IVC} increases due to the higher density of the trapped mass improving the environment where the combustion process develops in two ways, decreasing the equivalence ratio by increasing the fresh air availability and enhancing the spray mixing due to the higher density attained at the TDC.

An additional positive effect is observed is Figure 14 (right) considering the progressive reduction of T_{max} and p_{max}. If the engine calibration is adjusted to get a similar combustion process independently from the given T_{intake} (as it was assumed in these simulations), the lower T_{max} and p_{max} decreases the thermomechanical loads withstood by the engine, together with lower NO_x emission levels by decreasing also the flame temperatures.

According to Figure 15 (left) the potential benefit in indicated efficiency comparing the extreme T_{intake} cases is almost 4% in all operating conditions, and most of this benefit comes from the reduction of the heat rejected through the combustion chamber walls as included also in this figure. However, part of the energy gained due to the lower heat rejection flows with the exhaust gas. Figure 15 (right) also shows how despite the decrease of T_{exh} by around 100°C, H_{exh} increases as T_{intake} decreases as a consequence of the higher flow rate being exhausted that overcompensates the reduction of exhaust gas temperature.

Further analysis shows how an interesting option could be recalibrating the engine to keep the same T_{max} and p_{max} for all T_{intake} levels since in this case, the combustion can be better phased and/or faster, providing also benefits on engine indicated efficiency without important impacts on NO_x emissions. Both alternatives are expected to improve the NOx – ISFC trade-off.

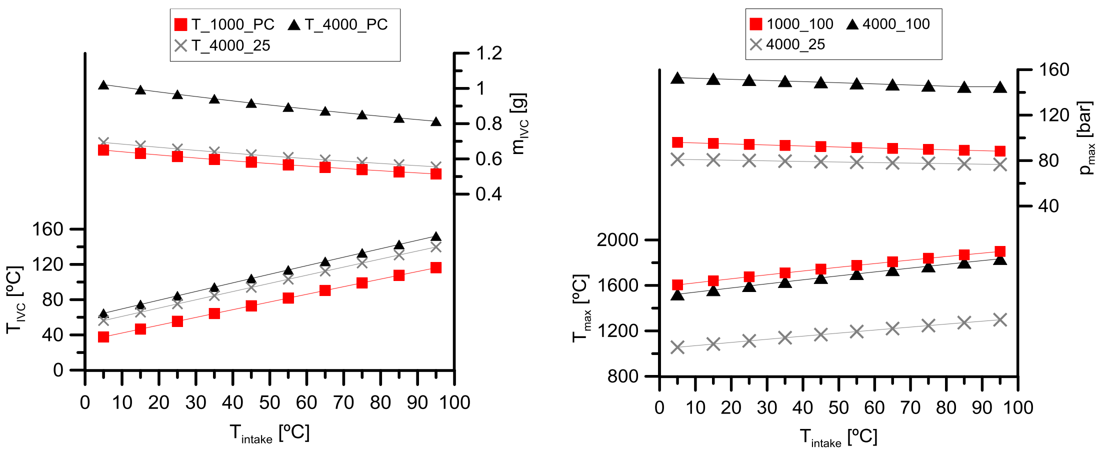

Figure 14. Effect of Ti_{ntake} on T_{IVC} and m_{IVC} (left), on T_{max} and p_{max} (right)

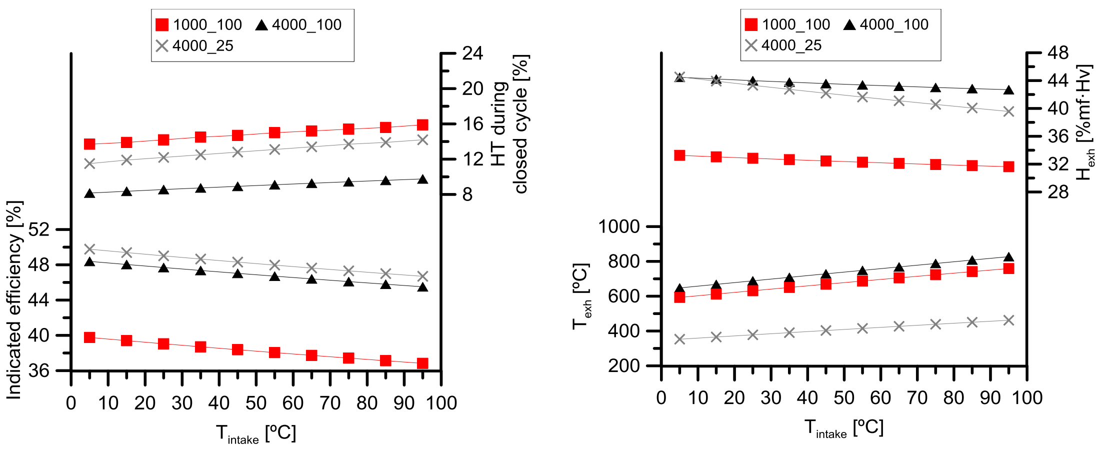

Figure 15. Effect of Ti_{ntake} on Indicated efficiency and HT during the closed cycle (left), on T_{exh} and H_{exh} (right)

These results from simulations encouraged the authors to test the effects of T_{intake} in the real engine. For the experimental assessment neither the intake conditions variation nor the operating condition were the same (at least in some points) as those used for the refrigeration cycle design. This redefinition of the validation points is imposed by the limitations of the experimental installation. Thus, the experimental facility does not include a real refrigeration cycle but a water-air heat exchanger cooled by an external water circuit. Hence, the limit for T_{intake} range are defined by the maximum compressor outlet temperature (with no water cooling at the exchanger) and the minimum T_{intake} achievable with the maximum coolant flow at the ambient temperature. As a consequence, the T_{intake} reduction must be adjusted at each operating point. Additionally, the T_{intake} range achievable at low engine speed was so small that it was discarded for the experimental validation.

Although the viability of the refrigeration cycle has been checked at high load, the worst condition with the less energy available in the exhaust gas flow was preferred for the experimental validation of the potential of this waste heat recovery concept in order to assure its feasibility in the complete engine map, especially considering that in urban driving conditions the engine operates mostly at low loads. In addition, evaluating the improvements provided by this waste heat recovery concept is more interesting at low loads also due to the intrinsic engine low efficiency caused by the high heat rejection to chamber walls in relative to the mechanical power. Therefore, taking into account the previous comments, three operating points of an engine speed sweep (from 2000 to 4000 rpm) and 25% of the load was measured. The main variables (measured and calculated) for the analysis are shown in Table 8.

As air availability in the chamber has important effects on the combustion development, in order to keep the same combustion profile as much as possible, the total trapped mass and fuel injected were kept constant during the tests. Thus, the intake pressure was reduced along with the intake temperature to maintain the mass flow. The injection settings were also fine-tuned to maintain the combustion phasing. Following this methodology the effects of intake temperature change can be analyzed to check the impact of decreasing heat rejection on performance and NOx – ISFC trade-off as much isolated as possible from those related to the combustion changes. As T_{intake} gap was different at the three operating conditions, these variations have been normalized to facilitate their comparison, thus the variation per 10 °C are shown in the last column of each operating condition. All the percentages refer to the fuel energy.

Results included in Figure 16 and Table 9 show how despite the slight differences at the three engine speeds, the general trends are very similar in all the cases. When T_{intake} decreases 10 °C both indicated and brake efficiencies improve between 0.11% and 0.19%, the heat rejection during closed cycle (Q_{cc}) diminishes about -0.3%, total heat rejected to coolant and oil (includes heat flux in the ports, in the chamber during open cycle and also friction) diminishes about -0.41% to -0.54%, exhaust enthalpy (H_g) gets lower between 0.43% to 0.63%. Regarding emissions, it is evident how reducing T_{intake} is a good solution to reduce NOx emissions but increases CO, while no clear effect was observed in the unburned hydrocarbon (HC).

As a final remark, the present research work confirms the feasibility of the waste heat recovery concept investigated, based on using the energy available in the exhaust gas to cool the intake flow by means of a bottoming absorption cycle, to improve the engine thermal efficiency in all the engine operating conditions from low to high speeds/loads. Additional benefits were also identified in terms of NOx emissions which are of great interest since its control by after-treatment systems is still challenging.

Table 8. Measured points for the validation

Variables	**2000[rpm]-25[%]**		**3000[rpm]-25[%]**		**4000[rpm]-25[%]**	
	Cold	**Hot**	**Cold**	**Hot**	**Cold**	**Hot**
T_{intake} [°C]	28	63	25	69	29	100
$T_{exhaust}$ [°C]	358	370	394	406	378	410
m_a [g/s]	33.2	33.2	47.5	48.0	74.5	74.2
m_f [g/s]	1.0	1.0	1.4	1.4	1.7	1.7
T_{cool} [°C]	86	85	86	86	85	85
T_{oil} [°C]	91	93	98	99	105	108

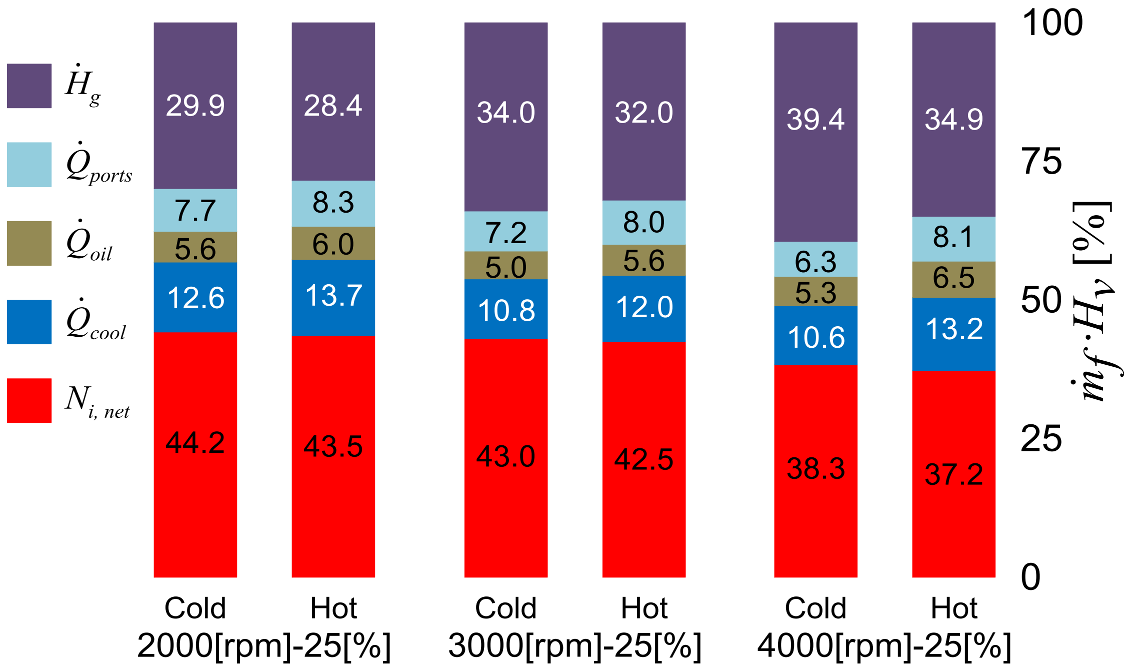

Figure 16. Energy split at intake temperature sweeps

Table 9. Averaged values

Variables	2000[rpm]-25[%]	3000[rpm]-25[%]	4000[rpm]-25[%]
	Δ(-10ºC)	Δ(-10ºC)	Δ(-10ºC)
Ind. Eff. [%]	0.19	0.19	0.11
Brake eff. [%]	0.12	0.11	0.12
Qcc [%]	-0.31	-0.28	-0.36
Ind. Eff./Qcc [%]	40.5	39.5	34.4
Qcool [%]	-0.32	-0.28	-0.37
Qoil [%]	-0.12	-0.13	-0.17
Qports [%]	-0.18	-0.17	-0.25
Hg [%]	0.43	0.45	0.63
NOx [ppm]	-42	-29	-32
HC [ppm]	2	4	0
CO [ppm]	33	59	24

5. CONCLUSIONS

This paper describes the thermodynamic analysis of a single-stage ARC using the solution NH_3-H_2O used to cool down the intake air of a turbocharged 1.6 l Turbocharged Diesel engine. Both simulations with the ARC and the engine were performed in parallel, considering independent systems with little interaction. Optimization and description of main parameters in an ARC were presented.

The following results have been obtained:

- The exhaust gases from an ICE was confirmed as a promising power source for ARC.
- There is enough power in the exhaust gases to operate the ARC in all the points of the engine map.
- ARC should operate between parameters optimized to ensure proper heat rejection to the ambient.
- A potential benefit in indicated efficiency of almost 4% is theoretically estimated in all operating conditions.
- From the theoretical analysis, it is clear how most of this benefit comes from the reduction of the heat rejected through the combustion chamber walls, while additional positive impact is associated to the increment in engine volumetric efficiency and total trapped mass into the combustion chamber.
- Experimental results confirm the predicted benefits in indicated efficiency even keeping constant the total trapped mass into the combustion chamber, so it is evident the key role of reducing the heat rejection as the main factor explaining the benefits observed in indicated efficiency.
- Regarding emissions, it is evident how reducing T_{intake} is a good solution to reduce NOx emissions but increases CO, while no clear effect was observed in the unburned hydrocarbon (HC).

This study can be a useful source to show the potential of this particular application. Future work will focus on the development of an experimental installation to test and confirm the results obtained from simulations.

Acknowledgements

Authors want to acknowledge the “Apoyo para la investigación y Desarrollo (PAID)” grant for doctoral studies (FPI S2 2015 1067).

References

[1] A. J. Torregrosa, A. Broath, P. Olmeda, and C. Romero, “Assessment of the influence of different cooling system configurations on engine warm-up, emissions and fuel consumption,” *Int. J. Automot. Technol.*, vol. 9, no. 4, pp. 447–458, 2008.

[2] H. Aghaali and H.-E. Ångström, “A review of turbocompounding as a waste heat recovery system for internal combustion engines,” *Renew. Sustain. Energy Rev.*, vol. 49, pp. 813–824, 2015.

[3] W. M. S. R. Weerasinghe, R. K. Stobart, and S. M. Hounsham, “Thermal efficiency improvement in high output diesel engines a comparison of a Rankine cycle with turbo-compounding,” *Appl. Therm. Eng.*, vol. 30, no. 14–15, pp. 2253–2256, 2010.

[4] V. Dolz, R. Novella, A. García, and J. Sánchez, “HD Diesel engine equipped with a bottoming Rankine cycle as a waste heat recovery system. Part 1: Study and analysis of the waste heat energy,” *Appl. Therm. Eng.*, vol. 36, no. 1, pp. 269–278, 2012.

[5] J. Galindo, S. Ruiz, V. Dolz, L. Royo-Pascual, R. Haller, B. Nicolas, and Y. Glavatskaya, “Experimental and thermodynamic analysis of a bottoming Organic Rankine Cycle (ORC) of gasoline engine using swash-plate expander,” *Energy Convers. Manag.*, vol. 103, pp. 519–532, 2015.

[6] J. R. Serrano, V. Dolz, R. Novella, and A. García, "HD Diesel engine equipped with a bottoming Rankine cycle as a waste heat recovery system. Part 2: Evaluation of alternative solutions," *Appl. Therm. Eng.*, vol. 36, no. 1, pp. 279–287, 2012.

[7] M. Bailey, "Comparative Evaluation of Three Alternative Power Cycles for Waste Heat Recovery from the Exhaust of Adiabatic Diesel Engines," *DOE NASA, United Technol. Res. Cent.*, vol. 86953, 1985.

[8] J. Galindo, J. Serrano, V. Dolz, and P. Kleut, "Brayton cycle for internal combustion engine exhaust gas waste heat recovery," *Adv. Mech. Eng.*, vol. 7, no. 6, pp. 1–9, 2015.

[9] J. C. Bass, A. S. Kushch, and N. B. Elsner, "Thermoelectric Generator (TEG) for Heavy Diesel Trucks John C. Bass, Aleksandr S. Kushch, Norbert B. Elsner Hi-Z Technology, Inc."

[10] A. S. Kushch, J. C. Bass, S. Ghamaty, and N. B. Eisner, "Thermoelectric development at Hi-Z technology," *Proc. ICT2001. 20 Int. Conf. Thermoelectr. (Cat. No.01TH8589)*, pp. 1–9, 2001.

[11] S. Wang, "A car air-conditioning system based on an absorption refrigeration cycle using energy from exhaust gas of an internal combustion engine," *J. Energy South. Africa*, vol. 19, no. 4, pp. 6–11, 2008.

[12] A. A. Manzela, S. M. Hanriot, L. Cabezas-Gómez, and J. R. Sodré, "Using engine exhaust gas as energy source for an absorption refrigeration system," *Appl. Energy*, vol. 87, no. 4, pp. 1141–1148, Apr. 2010.

[13] J. Koehler, W. J. Tegethoff, D. Westphalen, and M. Sonnekalb, "Absorption refrigeration system for mobile applications utilizing exhaust gases," *Heat Mass Transf.*, vol. 32, pp. 333–340, 1997.

[14] B. Agnew, M. Talbi, and M. Mostafavi, "Combined power and cooling, an analysis of the combined Diesel-absorption cycle," *Appl. Therm. Eng.*, vol. 19, no. 10, pp. 1097–1105, Oct. 1999.

[15] M. Talbi and B. Agnew, "Energy recovery from diesel engine exhaust gases for performance enhancement and air conditioning," *Appl. Therm. Eng.*, vol. 22, no. 6, pp. 693–702, Apr. 2002.

[16] S. L. Sowjanya, "Thermal Analysis of a Car Air Conditioning System Based On an Absorption Refrigeration Cycle Using Energy from Exhaust Gas of an Internal Combustion Engine," *Adv. Eng. Appl. Sci.*, vol. 3, no. 4, pp. 47–53, 2015.

[17] J. Liu and S. Xu, "The performance of absorption-compression hybrid refrigeration driven by waste heat and power from coach engine," *Appl. Therm. Eng.*, vol. 61, no. 2, pp. 747–757, 2013.

[18] A. T. Rêgo, S. M. Hanriot, A. F. Oliveira, P. Brito, and T. F. U. Rêgo, "Automotive exhaust gas flow control for an ammonia-water absorption refrigeration system," *Appl. Therm. Eng.*, vol. 64, no. 1–2, pp. 101–107, 2014.

[19] T. Zegenhagen and F. Ziegler, "Experimental investigation of the characteristics of a jet-ejector and a jet-ejector cooling system operating with R134a as a refrigerant," *Int. J. Refrig.*, vol. 56, pp. 173–185, 2015.

[20] M. T. Zegenhagen and F. Ziegler, "Feasibility analysis of an exhaust gas waste heat driven jet-ejector cooling system for charge air cooling of turbocharged gasoline engines," *Appl. Energy*, vol. 160, pp. 221–230, 2015.

[21] J. Patek and J. Klomfar, "Simple functions for fast calculations of selected thermodynamic properties of the ammonia-water system," *Int. J. Refrig.*, vol. 18, no. 4, pp. 228–234, 1995.

[22] P. Srikhirin and S. Aphornratana, “A review of absorption refrigeration technologies,” *Renew. Sustain. Energy Rev.*, vol. 5, pp. 343–372, 2001.

[23] I. Horuz, “A comparison between ammonia-water and water-lithium bromide solutions in vapor absorption refrigeration systems,” *Heat Mass Transf.*, vol. 25, no. 5, pp. 711–721, 1998.

[24] A. D. Althouse, C. H. Turnquist, and A. F. Bracciano, “Modern refrigeration and air conditioning. Theory, practice of refrigeration and air conditioning systems,” vol. -1, 1968.

[25] Y.-R. Li, J.-N. Wang, and M.-T. Du, “Influence of coupled pinch point temperature difference and evaporation temperature on performance of organic Rankine cycle,” *Energy*, vol. 42, no. 1, pp. 503–509, Jun. 2012.

[26] F. Payri, P. Olmeda, J. Martin, and R. Carreño, “A New Tool to Perform Global Energy Balances in DI Diesel Engines,” *SAE Int. J. Engines*, vol. 7, no. 1, pp. 43–59, 2014.

[27] F. Payri, J. M. Luján, J. Martín, and A. Abbad, “Digital signal processing of in-cylinder pressure for combustion diagnosis of internal combustion engines,” *Mech. Syst. Signal Process.*, vol. 24, no. 6, pp. 1767–1784, Aug. 2010.

[28] J. Tichý and G. Gautschi, *Elektrische Meßtechnik*. Berlin: Springer, 1980.